Charge Separation

International Edition: DOI: 10.1002/anie.201509067
German Edition: DOI: 10.1002/ange.201509067

Remarkable Dependence of the Final Charge Separation Efficiency on the Donor–Acceptor Interaction in Photoinduced Electron Transfer

Tomohiro Higashino, Tomoki Yamada, Masanori Yamamoto, Akihiro Furube, Nikolai V. Tkachenko, Taku Miura, Yasuhiro Kobori,* Ryota Jono, Koichi Yamashita,* and Hiroshi Imahori**

Abstract: *The unprecedented dependence of final charge separation efficiency as a function of donor–acceptor interaction in covalently-linked molecules with a rectilinear rigid oligo-p-xylene bridge has been observed. Optimization of the donor–acceptor electronic coupling remarkably inhibits the undesirable rapid decay of the singlet charge-separated state to the ground state, yielding the final long-lived, triplet charge-separated state with circa 100% efficiency. This finding is extremely useful for the rational design of artificial photosynthesis and organic photovoltaic cells toward efficient solar energy conversion.*

Photoinduced electron transfer (ET) is one of the most fundamental processes in physics, chemistry, and biology. In the reaction center of natural photosynthesis, photoinduced ET generates a long-lived charge separation (CS) state with circa 100% efficiency, leading to light-to-chemical energy conversion.[1] In contrast, photoinduced CS at the interfaces of organic photovoltaic cells and dye-sensitized solar cells generates an electron–hole pair, eventually achieving light-to-electricity conversion.[2] However, the interfaces of semiconductor–dye and donor–acceptor (D-A) in artificial photosynthesis and organic photovoltaic cells often suffer from the partial or even large loss of the CS state at the early stage, which is still controversial and not fully understood owing to inevitable inhomogeneous spatial distribution of D-A components.[3]

In this context, D-A linked systems have generated remarkable interest over the last few decades.[4] The D-A covalent linkage can eliminate complex factors arising from diffusion in solutions and assess the photoinduced ET properties precisely with the help of homogenous spatial distribution of the D-A components. So far, these systems have provided fundamental information on photoinduced ET. Impact of various ET parameters, such as driving force (ΔG^0_{ET}), electronic coupling (V), reorganization energy (λ), and temperature (T), on ET rate has been evaluated by using elaborated D-A linked molecules. In particular, a well-defined D-A linked molecule with a rigid bridge has allowed us to shed light on photoinduced ET more accurately.[5] Herein we show unprecedented dependence of the final CS efficiency (Φ_{CS}) on the D-A interaction (that is, electronic coupling) that can be changed systematically in the D-A linked models with a one-dimensional (1D) nonconjugated bridge. We have thoroughly examined the photoinduced ET properties by using femtosecond to microsecond time-resolved transient absorption (TRTA) and electron paramagnetic resonance (TREPR) spectroscopies.

In this study, we synthesized a systematic series of D-A linked molecules ZnP-xy$_n$-C$_{60}$ ($n = 1$–5) with discrete chemical structures to address the effect of electronic coupling on

[*] Dr. T. Higashino, T. Yamada, M. Yamamoto, Prof. Dr. H. Imahori
Department of Molecular Engineering
Graduate School of Engineering, Kyoto University
Nishikyo-ku, Kyoto, 615–8510 (Japan)
E-mail: imahori@scl.kyoto-u.ac.jp
Prof. Dr. A. Furube[+]
National Institute of Advanced Industrial Science and Technology (AIST)
Tsukuba Central 2, 1-1-1- Umezono, Tsukuba, Ibaraki 305–8568 (Japan)
Prof. Dr. N. V. Tkachenko
Department of Chemistry and Bioengineering
Tampere University of Technology
P.O.Box 541, 33101 Tampere (Finland)
E-mail: nikolai.tkachenko@tut.fi
T. Miura, Prof. Dr. Y. Kobori
Department of Chemistry, Graduate School of Science
Kobe University
1-1 Rokkoudai-cho, Nada-ku, Kobe 657–8501 (Japan)
E-mail: ykobori@kitty.kobe-u.ac.jp
Prof. Dr. Y. Kobori
PRESTO (Japan) Science and Technology Agency
Kawaguchi, Saitama 332-0012 (Japan)
Dr. R. Jono, Prof. Dr. K. Yamashita
Department of Chemical System Engineering
School of Engineering, The University of Tokyo
7-3-1, Hongo, Bunkyo-ku, Tokyo 113–8656 (Japan)
E-mail: yamasita@chemsys.t.u-tokyo.ac.jp
Prof. Dr. H. Imahori
Institute for Integrated Cell-Material Sciences (WPI-iCeMS)
Kyoto University
Nishikyo-ku, Kyoto 615–8510 (Japan)
[+] Present address: Institute of Technology and Science
Tokushima University
2-1, Minamijosanjima-cho, Tokushima, 770–8506 (Japan)

Supporting information and ORCHID(s) from the author(s) for this article are available on the WWW under http://dx.doi.org/10.1002/anie.201509067.

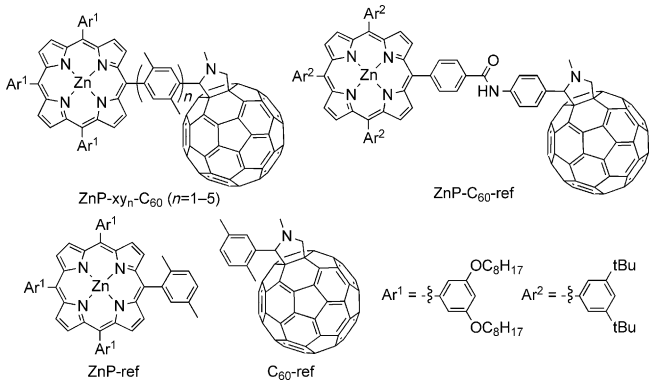

Figure 1. Molecular structures of CS molecules and reference compounds.

photoinduced CS and charge recombination (CR) as well as on Φ_{CS} (Figure 1). To assess the ET processes, zinc porphyrin (ZnP) as a donor and C_{60} as an acceptor were chosen owing to their excellent ET properties.[6] We also selected rectilinear rigid oligo-*p*-xylene bridges between ZnP and C_{60} because they are known to exhibit length-independent electronic structure, which is highly suitable for evaluating true distance dependence of tunneling coherent ET.[7] Details on the synthesis and characterization are provided in the Supporting Information. ZnP-C_{60}-ref,[8] ZnP-ref, and C_{60}-ref were also prepared as reference compounds (Figure 1).

The absorption spectrum of ZnP-xy$_2$-C_{60} in benzonitrile (PhCN) is shown in Figure 2a. The spectrum is almost the linear combination of those of ZnP-ref and C_{60}-ref, implying a negligible electronic interaction between ZnP and C_{60} in the ground state. Similar behavior is noted for ZnP-xy$_n$-C_{60} (n = 1,3–5; Supporting Information, Figure S1a). The peak positions and shapes of the absorption spectra are almost the same for all ZnP-xy$_n$-C_{60}, showing that π-conjugation through the bridge is virtually negligible for all dyads (Supporting Information, Table S1). The fluorescence of ZnP is quenched by C_{60} in ZnP-xy$_n$-C_{60}, suggesting the occurrence of ET and/or energy transfer (EN) from ZnP first excited singlet state (ZnP^{S1}) to C_{60} (Supporting Information, Figure S1b). With decreasing the number of the xylene unit the fluorescence is decreased gradually, reflecting the distance dependent attenuation of the ZnP fluorescence quenching by C_{60}.

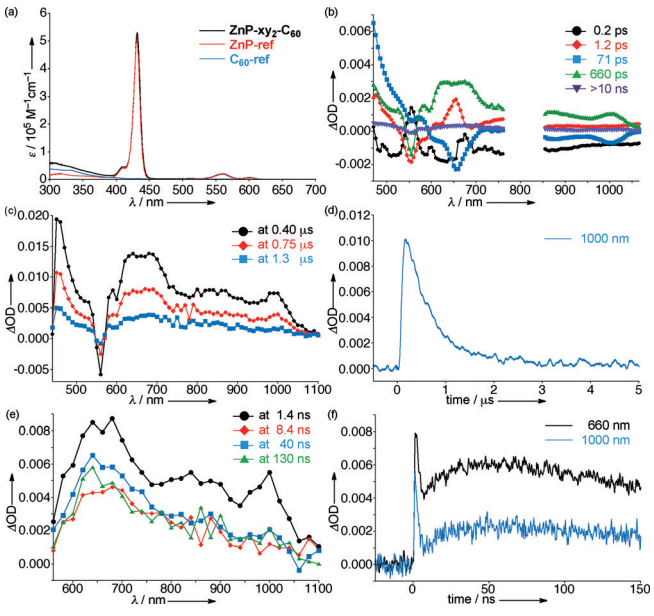

Figure 2. a) Absorption spectra of ZnP-xy$_2$-C_{60}, ZnP-ref, and C_{60}-ref in PhCN. b) Femtosecond to picosecond TRTA component spectra of ZnP-xy$_2$-C_{60}. c) Nanosecond to microsecond TRTA spectra of ZnP-xy$_2$-C_{60}. d) Time absorption profile at 1000 nm. e) Nanosecond TRTA spectra of ZnP-xy$_2$-C_{60}. f) Time absorption profiles at 660 nm and 1000 nm.

TRTA spectroscopy was performed for ZnP-xy$_n$-C_{60} with selective excitation of the ZnP chromophore. Figure 2b shows femtosecond to picosecond TRTA component spectra of ZnP-xy$_2$-C_{60} in PhCN obtained from global five-exponential fit of the data. The first and second components (τ = 0.2, 1.2 ps) can be assigned to the internal conversion (IC) from the ZnP second excited singlet state (ZnP^{S2}) to ZnP^{S1} associated with vibrational relaxation. The third component with negative absorption at 560, 600, and 660 nm can be attributed to the decay of ZnP^{S1} owing to the bleaching and stimulated emission of ZnP^{S1}. The fourth component with τ = 660 ps exhibits characteristic absorption of the ZnP radical cation (ZnP$^{\bullet+}$) at 600–700 nm and C_{60} radical anion ($C_{60}^{\bullet-}$) at 1000 nm,[8] corroborating the formation and decay of the CS state. Note that the final component with $\tau > 10$ ns reveals very weak absorption resembling the CS state, which has not been detected before (Supporting Information, Figure S2a). We also conducted nanosecond to microsecond TRTA measurements for ZnP-xy$_2$-C_{60} in PhCN. Surprisingly, the CS state, which seems to decay to the ground state with τ = 660 ps, still survives and recombines to the ground state with τ = 0.56 μs (Figures 2c,d). To shed light on the discrepancy between the TRTA behaviors in the different time regions, nanosecond TRTA measurements were carried out. The decay of the initial CS state cannot be probed completely because of the limit of the time resolution (a few ns), but the simultaneous rises of ZnP$^{\bullet+}$ at 600–700 nm and $C_{60}^{\bullet-}$ at 1000 nm with τ = 12 ns are evident (Figures 2e,f). From these results, we can conclude that the initially formed CS state with spin-singlet character decays to the ground state and/or is converted into the intermediate state, which is detected as the fifth component with the weak absorption in the picosecond TRTA measurement. Then, this intermediate, tentatively assigned as a triplet exciplex state, is further transformed with τ = 12 ns into the CS state with spin-triplet character (Figure 3a).[9] Similar results were obtained by revisiting the previously reported ZnP-C_{60}-ref (Supporting Information, Figure S3).[8] The photodynamics of ZnP-xy$_1$-C_{60} is largely comparable to those of ZnP-xy$_2$-C_{60} and ZnP-C_{60}-ref (Supporting Information, Figure S2). Nevertheless, owing to the stronger D-A electronic coupling, after IC from ZnP^{S2} to ZnP^{S1} (τ = 0.15 ps), the decay of ZnP^{S1} (τ = 1.6 ps) generates the singlet exciplex state, as seen in analogous ZnP-C_{60} linked molecules with one phenylene bridge.[10] The ZnP emission decays with τ = 2.2 ps, which is close to the TA decay rate. The exciplex state is transformed with τ = 12 ps into the singlet CS state and then seems to decay with τ = 132 ps to the ground

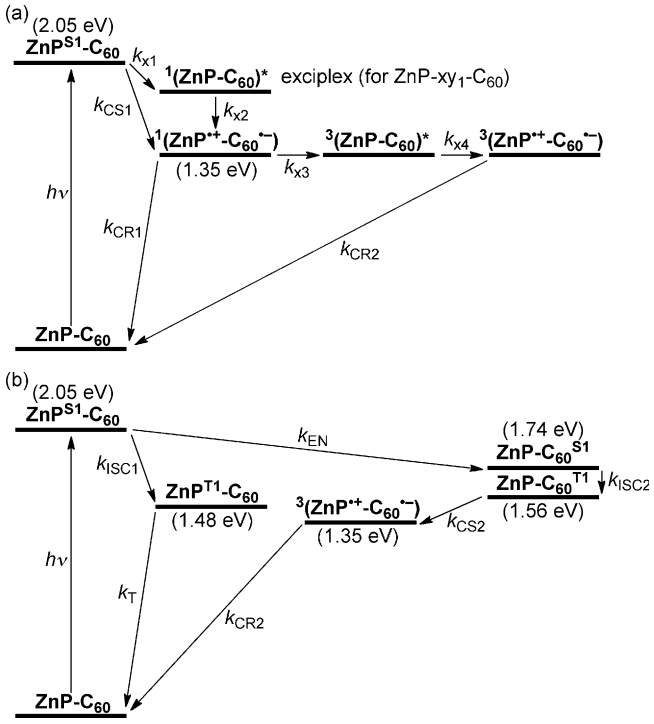

Figure 3. Relaxation pathways of a) ZnP-xy$_n$-C$_{60}$ ($n=1,2$) and ZnP-C$_{60}$-ref and b) ZnP-xy$_n$-C$_{60}$ ($n=3$–5) in PhCN.

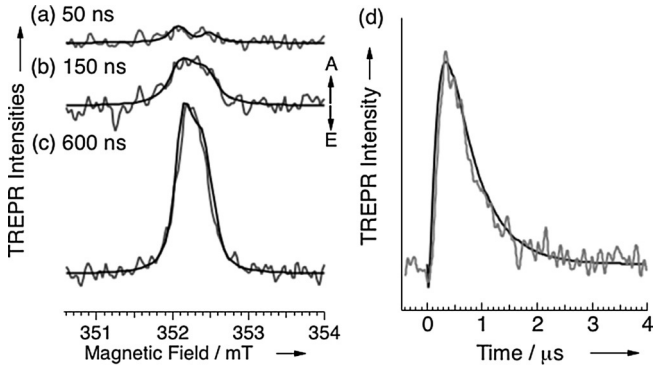

Figure 4. TREPR spectra of the ZnP$^{\bullet+}$-xy$_2$-C$_{60}^{\bullet-}$ state with the delay time of a) 50 ns, b) 150 ns, and c) 600 ns, obtained by the 420 nm laser irradiations of ZnP-xy$_2$-C$_{60}$ in PhCN at room temperature. d) The delay time dependence of the TREPR signal at $B_0=352.3$ mT. The fitting lines in (a)–(d) were obtained using the triplet-precursor electron spin polarization transfer model taking into account ^{3}(ZnP-xy$_2$-C$_{60}$)*→ ^{3}(ZnP$^{\bullet+}$-xy$_2$-C$_{60}^{\bullet-}$).

state in the femto to picosecond TRTA measurement. However, the significant triplet CS state is detectable in the nanosecond to microsecond TRTA measurement, suggesting the partial conversion of the singlet CS state to the triplet CS one via the triplet exciplex state (Figure 3a). As seen in the photophysics of ZnP-xy$_1$-C$_{60}$, ZnP-xy$_2$-C$_{60}$, and ZnP-C$_{60}$-ref in PhCN, the ZnP^{S1} moiety is strongly quenched by the C$_{60}$ moiety, generating the singlet CS state exclusively via photoinduced ET. Moreover, the energy level of the singlet CS state in PhCN (1.35 eV) is significantly lower than that of the ZnP first excited triplet state (ZnP^{T1}, 1.48 eV). This supports that the formation of the ZnP^{T1} state from the ZnP^{S1} state via the intersystem crossing (ISC) is very minor, if any, ruling out the possibility of CS from the ZnP^{T1} state.

To characterize the longer-lived CS state generated by the efficient second CS following the short-lived singlet CS state, we have observed X-band TREPR spectra by the 420 nm laser irradiations of ZnP-xy$_2$-C$_{60}$ in PhCN at room temperature (Figure 4). The microwave absorption (A) signals rise within 0.3 µs after the laser flash and decay with a lifetime shorter than 1 µs (Figure 4d). This profile is well consistent with the nanosecond to microsecond TRTA decay (Figure 2d and Table 1) of the CS state. Thus, the EPR signal is assigned to the triplet CS states generated after spin–lattice relaxations in the spin sublevels, resulting in the absorptive thermal equilibrium spin populations (see the Supporting Information for details). From Figure 2b, the primary singlet CS state is quickly deactivated within 1 ns to generate the triplet exciplex. This denotes that the spin–orbit coupling (SOC) plays a role on the CR as has been demonstrated by Wasielewski et al. for a ZnP–tetracyanonaphthoquinodimethane (TCNQD) linked system in which

Table 1: ET and related parameters of ZnP-xy$_n$-C$_{60}$ and ZnP-C$_{60}$-ref in PhCN.

	ZnP-xy$_1$-C$_{60}$	ZnP-xy$_2$-C$_{60}$	ZnP-xy$_3$-C$_{60}$	ZnP-xy$_4$-C$_{60}$	ZnP-xy$_5$-C$_{60}$	ZnP-C$_{60}$-ref
R_{ee}/Å	6.7	10.9	15.1	19.5	23.8	13.0
k_{x1}/s^{-1}	6.3×10^{11}	–	–	–	–	–
k_{x2}/s^{-1}	8.3×10^{10}	–	–	–	–	–
k_{x4}/s^{-1}	–	8.3×10^{7}	–	–	–	6.7×10^{7}
k_{CS1}/s^{-1}	–	1.4×10^{10}	–	–	–	1.5×10^{10}
k_{CS2}/s^{-1}	–	–	6.3×10^{7}	n.d.[a]	–	–
$k_{CR1}+k_{x3}$/s^{-1}[b]	7.6×10^{9}	1.5×10^{9}	–	–	–	1.3×10^{9}
k_{CR2}/s^{-1}	1.9×10^{6}	1.8×10^{6}	6.3×10^{5}	4.3×10^{5}	–	1.5×10^{6}
λ/eV	0.58	0.62	0.66	0.72	–	0.62
V/cm^{-1}	18	6.2	2.0	0.65	–	6.0
Φ_{CS}[c]/%	9.4 (8.1)	74 (64)	53 (46)	31 (27)	ca. 0 (ca. 0)	99[d] (85)[e]

[a] The ET rate constant could not be determined because of the overlapping of fluorescence in the nanosecond to microsecond measurement. [b] Although the rate constants for the decay of the singlet CS state ($k_{CR1}+k_{x3}$) were determined, those for the formation of the triplet exciplex state from the singlet CS state (k_{x3}) could not be obtained owing to the very weak absorption. [c] First, the relative Φ_{CS} values were determined in PhCN by comparing the absorbance of C$_{60}^{\bullet-}$ under the identical absorbance at the excitation wavelength (410 nm) where ZnP is selectively excited. Then, the absolute Φ_{CS} values were obtained on the basis of the absolute Φ_{CS} values of ZnP-C$_{60}$-ref in PhCN. [d] The absolute Φ_{CS} value of ZnP-C$_{60}$-ref in PhCN (99%) was determined by photocatalytic oxidation of 1-benzyl-1,4-dihydronicotinamide (BNAH) by hexyl viologen (HV^{2+}) in the presence of ZnP-C$_{60}$-ref in deoxygenated PhCN at the excitation wavelength (433 nm) where ZnP is selectively excited.[13] [e] The absolute Φ_{CS} value of ZnP-C$_{60}$-ref in PhCN (85%) was determined by TA measurement in deoxygenated PhCN at the excitation wavelength (532 nm) where ZnP is selectively excited.[8a] These values are listed in parentheses.

in-plane triplet sublevels were directly populated in the ZnP^{T1} moiety by the SOC-induced CR from the singlet CS state.[11a] In the present system, the unpaired orbital in $C_{60}^{\bullet-}$ possesses the p-orbital components orienting to several directions because of the spherical spin distribution in the C_{60} moiety. Thus, during the CR process to yield the π^* orbital of the $^3\pi\pi^*$ character in ZnP^{T1} from $C_{60}^{\bullet-}$ to $ZnP^{\bullet+}$, certain angular momentum changes are expected to be accompanied along the X and Y principal axes (for in-plane directions in ZnP^{T1}, see the Supporting Information, Figure S4) in the spin–spin dipolar coupling in ^{3}(ZnP-xy$_2$-C$_{60}$)*.[11b] Here we consider the triplet populations of $(p_X{:}p_Y{:}p_Z) = (0.44{:}0.44{:}0.12)$ for the zero-field spin sublevels (X, Y, and Z, respectively) in the precursor triplet exciplex dominated by ZnP^{T1}-xy$_2$-C$_{60}$ assuming the dipolar coupling parameters of $D = +0.030$ cm^{-1} and $E = +0.001$ cm^{-1} (see the Supporting Information). Using the triplet electron spin polarization transfer (ESPT) model,[11c] we have computed the delay time dependence of the TREPR signals of the CS state (the fitted lines in Figure 4) initiated by the SOC-induced CR. The good agreements have been obtained in Figure 4 by employing the dyad geometry shown in the Supporting Information, Figure S4. This result complemented the characteristics of the triplet CS state supporting the sequential transformation to the triplet CS state via the triplet exciplex state generated from the short-lived singlet CS state (Figure 3a; see the Supporting Information, Figure S4 for details).

By increasing the number of the xylene unit from $n = 2$ to $n = 3$, the relaxation pathway is altered greatly (Figure 3b). In the case of ZnP-xy$_3$-C$_{60}$ in PhCN, a three-exponential global fit is sufficient to analyze the femtosecond to picosecond TRTA (Supporting Information, Figure S5a). The first component with $\tau = 1.5$ ps is attributable to IC from ZnP^{S2} to ZnP^{S1}. The second component has distinct negative absorption at 560, 600, and 660 nm and lifetime $\tau = 870$ ps, which agrees with the fluorescence lifetime (790 ps) and thus can be assigned to the decay of ZnP^{S1}. Given the fluorescence lifetime of ZnP-ref (1.70 ns), the additional relaxation channel has $\tau = 1.78$ ns. Thus, 51% of ZnP^{S1} undergoes ISC to generate the ZnP^{T1} state. ZnP^{T1} decays to the ground state without yielding the triplet CS state, which agrees with the final CS efficiency (see below). The electronic coupling for CS from the ZnP^{T1} state to the C_{60} moiety would not be sufficient for the occurrence of the CS owing to the insufficient overlap of π orbitals between the planar porphyrin and xylene spacer by the orthogonal geometry. The relaxation channel for the rest of 49% can be either ET or EN from ZnP^{S1} to C_{60}. Considering that ET rate is reduced more rapidly than EN rate with an increase in the D-A separation distance together with the almost the same fluorescence lifetime in toluene and PhCN, EN rather than ET would prevail. Nanosecond TRTA reveals the characteristic absorption derived from ZnP^{T1} at 850 nm, C_{60} first excited triplet state (C_{60}^{T1}) at 700 nm, and $C_{60}^{\bullet-}$ at 1000 nm (Supporting Information, Figure S5d,e). By analyzing the rise of absorption at 660 nm, ET from ZnP to C_{60}^{T1} takes place with $\tau = 16$ ns. Nanosecond to microsecond TRTA measurement exhibits the decay of the triplet CS state with $\tau = 1.6$ μs (Supporting Information, Figure S5b,c). Analogous, but less efficient EN from ZnP^{S1} to C_{60}, followed by ISC and CS from ZnP to C_{60}^{T1} is noted for ZnP-xy$_4$-C$_{60}$ (Supporting Information, Figures S6 and S7).[12] The photodynamics of ZnP-xy$_5$-C$_{60}$ is almost identical to that of ZnP-ref, demonstrating little or no occurrence of ET and EN in ZnP-xy$_5$-C$_{60}$ (Supporting Information, Figure S8).

To quantify the ΔG^0_{ET} dependence on the ET rate constants (k_{ET}), Equation (1) was employed, where k_B is the Boltzmann constant and h is the Planck constant.[8b]

$$k_{ET} = \left(\frac{4\pi^3}{h^2\lambda k_B T}\right)^{1/2} V^2 exp\left[-\frac{(\Delta G^0_{ET} + \lambda)^2}{4\lambda k_B T}\right] \quad (1)$$

The ΔG^0_{ET} values were electrochemically determined in different polar solvents by using ZnP-ref and C_{60}-ref, whereas the k_{ET} values were also measured in the same solvents (Supporting Information, Tables S2–S4).[8b] The ET parameters obtained by Equation (1) are listed in Table 1 (Supporting Information, Figure S9). With an increase in the R_{ee} value, the λ values are increased, while the V values are decreased gradually. The distance dependence of V is frequently described by Equation (2), where V_0 is a maximal electronic coupling and β is a decay coefficient (damping factor) that depends on the nature of the bridge, energy gap between the HOMO or LUMO level of the bridge and D or A, and electronic coupling between D or A and the bridge.

$$V^2 = {V_0}^2 \exp(-\beta R_{ee}) \quad (2)$$

The β value is calculated to be 0.52 Å^{-1} (Supporting Information, Figure S10), which is comparable with the previously reported β values of 0.52 and 0.77 Å^{-1} for oligo-*p*-xylene bridge.[7] Finally, we estimated the Φ_{CS} value of the triplet CS state by comparing the absorbance of $C_{60}^{\bullet-}$ under the identical absorbance at $\lambda_{ex} = 410$ nm. With a decrease in the electronic coupling the Φ_{CS} value is increased dramatically and reaches a maximum of 99% for ZnP-C_{60}-ref[13] and then drops rapidly. The decreasing trend for $n = 3$–5 can be interpreted by slowing down the EN rate from ZnP^{S1} to C_{60}, and thus increasing yield of ZnP^{T1}, which does not contribute to intramolecular CS. To rationalize this large gap in the CS efficiency in the region of relatively strong D-A electronic coupling, theoretical calculations for the electronic coupling between the singlet CS state (^{1}CS) and the ground state (^{1}GS) were performed. The electronic coupling for ZnP-xy$_1$-C$_{60}$ is much larger than that for ZnP-xy$_2$-C$_{60}$, supporting the remarkably smaller Φ_{CS} value of ZnP-xy$_1$-C$_{60}$ compared to that of ZnP-xy$_2$-C$_{60}$ (Supporting Information, Figure S11).

This dramatic dependence of the Φ_{CS} value on the electronic coupling highlights the importance of tuning electronic coupling for optimizing final CS efficiency. At the short D-A separation distance (R_{ee}), the initially formed singlet CS state decays to the ground state and/or is competitively converted into a newly found intermediate state (that is, triplet exciplex), which is further transformed into the triplet CS state. Optimization of the D-A interaction remarkably inhibits the undesirable rapid decay to the ground state, yielding the final long-lived triplet CS state with circa 100% efficiency. This also raises an alarm over the conventional interpretation of frequently observed undesirable fast

CR in term of semi-classical Marcus theory for ET, which has been explained by the strong vibration-ET coupling.[14] This could be associated with the evolution of the barely detectable triplet exciplex state, which would govern the fate of the relaxation, that is, decaying directly to the ground state versus generating the triplet CS state. These unprecedented finding on the final CS efficiency, which is accessible only from the present models, will give us a practical blueprint for highly efficient artificial photosynthesis and organic photovoltaic cells by fine-tuning of donor–acceptor interaction.

Acknowledgements

This work was supported by WPI Initiative, MEXT, Japan. This research was also supported by Grand-in-Aid (No. 25220801 to H.I.). A part of this work was conducted at the Nano-Processing Facility, supported by IBEC Innovation Platform, AIST.

Keywords: charge separation · electron transfer · electronic coupling · exciplexes · Marcus theory

How to cite: *Angew. Chem. Int. Ed.* **2016**, *55*, 629–633
Angew. Chem. **2016**, *128*, 639–643

[1] R. E. Blankenship, *Molecular Mechanisms of Photosynthesis*, Wiley-Blackwell, Chichester, **2001**.
[2] a) S. Günes, H. Neugebauer, N. S. Sariciftci, *Chem. Rev.* **2007**, *107*, 1324–1338; b) A. Hagfeldt, G. Boschloo, L. Sun, L. Kloo, H. Pettersson, *Chem. Rev.* **2010**, *110*, 6595–6663.
[3] a) T. Umeyama, H. Imahori, *J. Phys. Chem. C* **2013**, *117*, 3195–3209; b) H. Imahori, S. Kang, H. Hayashi, M. Haruta, H. Kurata, S. Isoda, S. E. Canton, Y. Infahsaeng, A. Kathiravan, T. Pascher, P. Chávera, A. P. Yartsev, V. Sundström, *J. Phys. Chem. A* **2011**, *115*, 3679–3690; c) A. Rao, P. C. Y. Chow, S. Gélinas, C. W. Schlenker, C.-Z. Li, H.-L. Yip, A. K.-Y. Jen, D. S. Ginger, R. H. Friend, *Nature* **2013**, *500*, 435–439; d) A. E. Jailaubekov, A. P. Willard, J. R. Tritsch, W.-L. Chan, N. Sai, R. Gearba, L. G. Kaake, K. J. Williams, K. Leung, P. J. Rossky, X.-Y. Zhu, *Nat. Mater.* **2013**, *12*, 66–73.
[4] a) M. R. Wasielewski, *Chem. Rev.* **1992**, *92*, 435–461; b) D. Gust, T. A. Moore, A. L. Moore, *Acc. Chem. Res.* **2001**, *34*, 40–48; c) D. M. Guldi, *Phys. Chem. Chem. Phys.* **2007**, *9*, 1400–1420; d) S. Fukuzumi, *Phys. Chem. Chem. Phys.* **2008**, *10*, 2283–2297.
[5] a) W. Davis, W. Svec, M. Ratner, M. Wasielewski, *Nature* **1998**, *396*, 60–63; b) M. Natali, S. Campagna, F. Scandola, *Chem. Soc. Rev.* **2014**, *43*, 4005–4018; c) M. U. Winters, E. Dahlstedt, H. E. Blades, C. J. Wilson, M. J. Frampton, H. L. Anderson, B. Albinsson, *J. Am. Chem. Soc.* **2007**, *129*, 4291–4297; d) J. Sukegawa, C. Schubert, X. Zhu, H. Tsuji, D. M. Guldi, E. Nakamura, *Nat. Chem.* **2014**, *6*, 899–905.
[6] H. Imahori, *Bull. Chem. Soc. Jpn.* **2007**, *80*, 621–636.
[7] O. S. Wenger, *Chem. Soc. Rev.* **2011**, *40*, 3538–3550.
[8] a) C. Luo, D. M. Guldi, H. Imahori, K. Tamaki, Y. Sakata, *J. Am. Chem. Soc.* **2000**, *122*, 6535–6551; b) H. Imahori, K. Tamaki, D. M. Guldi, C. Luo, M. Fujitsuka, O. Ito, Y. Sakata, S. Fukuzumi, *J. Am. Chem. Soc.* **2001**, *123*, 2607–2617.
[9] a) S.-H. Lee, A. G. Larsen, K. Ohkubo, Z.-L. Cai, J. R. Reimers, S. Fukuzumi, M. J. Crossley, *Chem. Sci.* **2012**, *3*, 257–269; b) F. Nastasi, F. Puntoriero, M. Natali, M. Mba, M. Maggini, P. Mussini, M. Panigati, S. Campagna, *Photochem. Photobiol. Sci.* **2015**, *14*, 909–918.
[10] a) T. J. Kesti, N. V. Tkachenko, V. Vehmanen, H. Yamada, H. Imahori, S. Fukuzumi, H. Lemmetyinen, *J. Am. Chem. Soc.* **2002**, *124*, 8067–8077; b) N. V. Tkachenko, H. Lemmetyinen, J. Sonoda, K. Ohkubo, T. Sato, H. Imahori, S. Fukuzumi, *J. Phys. Chem. A* **2003**, *107*, 8834–8844.
[11] a) M. R. Wasielewski, D. G. Johnson, W. A. Svec, K. M. Kersey, D. W. Minsek, *J. Am. Chem. Soc.* **1988**, *110*, 7219–7221; b) Z. E. X. Dance, Q. Mi, D. W. McCamant, M. J. Ahrens, M. A. Ratner, M. R. Wasielewski, *J. Phys. Chem. B* **2006**, *110*, 25163–25173; c) Y. Kobori, M. Fuki, H. Murai, *J. Phys. Chem. B* **2010**, *114*, 14621–14630.
[12] F. D'Souza, G. R. Deviprasad, M. E. Zandler, V. T. Hoang, A. Klykov, M. VanStipdonk, A. Perera, M. E. El-Khouly, M. Fujitsuka, O. Ito, *J. Phys. Chem. A* **2002**, *106*, 3243–3252.
[13] S. Fukuzumi, H. Imahori, K. Okamoto, H. Yamada, M. Fujitsuka, O. Ito, D. M. Guldi, *J. Phys. Chem. A* **2002**, *106*, 1903–1908.
[14] *Electron Transfer from Isolated Molecules to Biomolecules* (Eds.: J. Jortner, M. Bixon), Wiley, New York, **1999**.

Received: September 27, 2015
Revised: November 4, 2015
Published online: November 26, 2015

